Physical Sciences, Life Science and Engineering Volume: 2, Number 1, 2024, *Page*: 1-14

CFD Analysis of Operation Variables Impact on Microwave-Assisted Water Heating

Muataz Mohammed Sulaiman[1*], Ahmed Amer Al-Salman[2]

[12] Department of Chemical Engineering, College of Engineering, University of Babylon, Hilla, Iraq

DOI:
https://doi.org/10.47134/pslse.v2i1.318
*Correspondence: Muataz Mohammed Sulaiman
Email:
eng.moataz.alchalabi@uobabylon.edu.iq

Received: 23-10-2024
Accepted: 23-11-2024
Published: 24-12-2024

Abstract: *Microwaves are the best technique for thermal sensitive materials processes performing high temperature with short time and less consumption of energy in addition to perfect control. Microwave heating technique has a faster heating rate compared to conventional heating methods. Microwave process consists QVF tube of 240 mm length and 17 mm internal diameter which located in the center of microwave oven (2.45GHz). The experiments involve the flow rate of the water is (2, 4, and 6) l/hr and the power of the oven are (500, 750, 1000, and 1250) W. The temperature of the water increased by increasing power of microwaves and reached 110 ˚C at 1250 W and 2 l/hr flowrate and it is increased with decreasing of flowrates. The experimental temperature measured by inferred camera. The temperature predicted by COMSOL are aligned closely at power 500 W and all flow rate. The results were analysed by COMSOL Multiphysics (v6.0).*

Keywords: *Microwaves, Water Heating, Numerical Analysis Electromagnetic Field, Electrical Field, COMSOL*

Introduction

Microwave heating is superior to conventional heating due to rapidity of energy transfer, thermal efficiency, energy conservation characteristics, and ease temperature control(Cao et al., 2018). The utilization of microwaves as alternative heat sources has become more prevalent in both the residential and industrial sectors (Yeong et al., 2017). Microwave heating is an exceptional technique of heating (Liang et al., 2020). One of the greatest benefits of microwaves is characteristic as volumetric heating (Gao et al., 2019), In situations involving rapid heat transfer from the surface of an object to its interior capacity, microwaves swiftly convent the thermal energy of materials within the volume (Ahmed & Theydan, 2014). The fast heating of microwave technique reduce the surface area of heating and the process time (Yeong et al., 2017).

Thermal processing, which employs microwaves as an energy source, is a widely recognized and feasible substitute for rapidly processing thermo-sensitive materials at high temperatures for shorter durations (Salvi et al., 2011). The potential application of

microwave heating in surimi product manufacturing stems from the fact that the rapid heating rate would facilitate the rapid passage of surimi gel through the gel-cracking zone, thereby avoiding the "modori phenomenon" (gel thermal degradation) (Ohkubo et al., 2005). In the second phase, substituting microwave heating for conventional water bath heating substantially enhances gel strength and water retention capacity while conserving energy in comparison to the conventional heating approach (Cao, 2018), (Ji et al, 2016)

Uneven heating of a liquid passing through a tube within a microwave chamber can be mitigated through the implementation of resonant cavity continuous flow focused microwave systems and other emerging technologies. This is accomplished through the application of an electric field that follows an optimal circulation pattern, with its peak intensity located at the center of the tube (higher velocity), and its minimum intensity at the extremities of the tube (lower velocity)(Salvi et al., 2011).

The comprehension of the three-dimensional temperature profile distribution of heated tube is of utmost importance in order to optimize microwave heating processes (Knoerzer et al., 2006). The temperature of the heated product measured experimentally and determined numerically. All the temperature measuring devices reading are interference with the electromagnetic field so infrared camera was used. All the data was treated by numerical methodologies to predict the temperature from video's produced by infrared camera.

Comparatively to solid specimens that have been microwave-treated, the analysis of liquid samples is considerably more challenging due to the inherent fluid motion. The consequence of heating would interplay among flow fields, electromagnetic fields, and temperature profiles within the liquid (Yeong et al., 2017).

Nevertheless, one major limitation that prevents the progress of microwave technology is the inconsistent dispersion of heat within a water as a result of irregular electric field configurations(Liang et al., 2020). To mitigate the occurrence of an inconsistent heating pattern, household microwave ovens employ rotating glass turntable plates to facilitate the rotation of foods while they are being heated. Nevertheless, this approach might not be viable in industrial settings where the machinery is not specifically designed to rotate. Therefore, natural heat convection in the sample must be investigated in order to gain a deeper comprehension of microwave dielectric heating phenomena.(Yeong et al., 2017).

Another notable feature of microwave heating is its exceptional selectivity in the absorption of energy. Just polar substances were capable of effectively absorbing microwave energy and being heated. Increasing the polarity of a substance facilitates its susceptibility to heating (Lee, 2024a).

Polarization in the context of an electromagnetic field is represented by the permittivity of a substance. Polarity is commonly denoted in the microwave-assisted chemical industry through the utilization of relative permittivity as opposed to permittivity itself. Relative permittivity is calculated as the product of absolute permittivity and

permittivity in a vacuum environment. Alternating electric fields, on the other hand, utilize complex permittivity, which is represented by the following equation (Gao et al., 2019).

$$\varepsilon^* = \varepsilon' - j\varepsilon'' \qquad \text{Eq. (1)}$$

ε^* (perimeter of complex permittivity) is temperature and frequency dependent. The equation (1) illustrates that the complex permittivity consists of a real and an imaginary component (Cao, 2018). The real component, denoted as ε', signifies the polarizability of a substance and can be defined as its capacity to keep electromagnetic energy. The fictitious component, denoted as ε'', signifies the capability of converting microwave energy into thermal energy. Consequently, materials that experience distinct temperature increases due to microwave irradiation have notably distinct complex permittivity profiles (Al-Mashhadani et al., 2023).

In recent years, microwave radiation has been widely applied in chemical processes including chemical catalysis, organic synthesis, extraction, desiccation, evaporation, and drying, among others, as a prospective heating technique (Chan et al., 2014). Furthermore, in order to differentiate between polar and nonpolar compounds, it has devised a microwave-induced evaporation technique that operates on the principles of an imbalanced process (Li et al., 2019). However, controlling the distribution of electric fields is difficult for industrial applications, and research on microwave cavity design is scarce. Consequently, it is critical to establish unambiguity regarding the proper utilization of microwave applicators and the manner in which microwave heating should be implemented (Gao et al., 2019).

Scholars have encountered challenges when attempting to develop precise numerical models for the continuous microwave heating of water. The simultaneous solution of microwaves process is depend on three sets of equations which are Maxwell's equations, Fourier's energy balance equation, and the Navier–Stokes equation (Salvi et al., 2011).

Methodology

Laboratory scale microwave system was designed and tested for continuous flow water heating system as shown in Figure 1. The QVF tube (17 mm diameter and 240 mm length) was used for water heating in controlled a microwave system, and the evaporated water were cooled in a stainless-steel double-pipe heat exchanger. Once the vapor has been condensed then collected in storage tank (Maaroof, 2024).

Overall, the system can be categorized according to the type of flow and power. The studied range of water flow rate are (2, 4, and 6) l/hr and the power are (500, 750, 1000, and 1250) W.

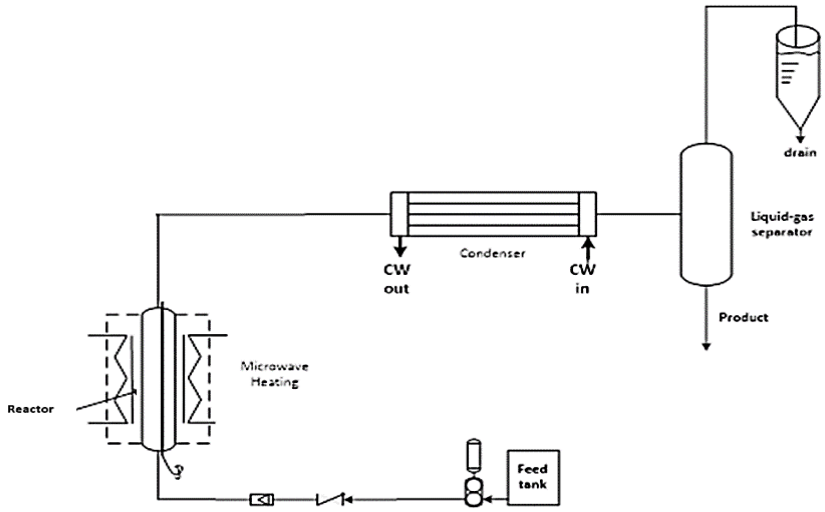

Fig 1. Unit Design Flowchart

Numerical

1. Solution (Model Description)

The COMSOL Multiphysics software offers a robust interactive environment that caters to an extensive array of scientific and engineering challenges. The utilization of COMSOL Multiphysics enables the seamless conversion of traditional models that depict a singular form of physics into multiphysics models that possess the ability to resolve coupled physical phenomena (Hong et al., 2016).

The main aim of our investigation was to develop a computational model that integrated phase transition and temperature-dependent characteristics using COMSOL. Experimental temperature profiles were employed to validate the simulated results for Newtonian and non-Newtonian fluids, with the intention of enhancing comprehension of the process. COMSOL Multiphysics v6.0 is utilized to conduct the computational simulation of microwave-induced water heating. The COMSOL model incorporates heat transfer in the domain of heat transfer, laminar flow, and heat transfer in the frequency domain for electromagnetic waves. Maxiwell's equations are utilizing the radio frequency module, while the Fourier and Navier Stokes equations are utilizing the heat transfer and fluid flow modules, respectively. The temperature field is ascertained through the integration of the heat transfer and fluid flow modules with the radio frequency module and the heat generation terms that are computed by the radio frequency module. Since the characteristic time scales of convective heat transfer processes and microwave dynamics differ by orders of magnitude, this three-way coupled conjugate problem permits weak (sequential) coupling (al-okbi et al., 2021).

COMSOL is predominantly founded on the finite element method (FEM) and is highly suitable for electromagnetics, occasionally encounters convergence challenges when applied to hydrodynamics problems. Furthermore, configuring COMSOL for acceptable

solution time and precision is typically more challenging in this domain. In the case of transient fluid flow dominated by advection, particularly those that are extremely tumultuous, the finite volume method (FVM) is more commonly used the finite element method (FEM) due to its reputation for greater robustness.(Vencels, Birjukovs, et al., 2019).

Package of proprietary software COMSOL Multiphysics is one of several software packages that offer pre-installed capabilities to address challenges related to coupled electromagnetics and hydrodynamics. Regarding open-source software, Elmer library couples was employed (Vencels, Råback, et al., 2019).

The schematic representation in Figure 1 depicts the progression of the heating mechanism that takes place within a microwave cavity. For the computation of the distributed heat source, a frequency-domain electromagnetic analysis at rest is utilized. The microwave cavity is a metallic structure measuring 400 (w) by 435 (d) by 260 (h). A 2.45 GHz microwave source is connected to the cavity via its exterior face. The 1500 W microwave receives input via the rectangular inlet located on the waveguide. QVF is employed in the fabrication of the dual concentric cylinder casings situated at the cavity's center. The cylinders have a length of 240 mm and a diameter of 17 mm. The QVF tube is distinguished by its transparency as a microwave medium (Zhang, 2024).

Table 1. the thermophysical properties of water

Property	Value
Relative permittivity (2.45 GHz, 293.15 K)	80.2
Relative permeability	1
Density (kg/m^3)	1000
Heat capacity (J/kg.K)	4190
Conductivity (S/m)	5.5 * 10^{-6}

It is generally accepted that the thermoelectric and dielectric properties of water remain constant with increasing temperature [27]. Table 1 contain the water properties in the simulation [28]. Therefore, the following assumptions are put forward, all of which fall within the acceptable range [2]:

1. The process of microwave absorption by the air within a microwave's cavity is minimum.
2. The microwave oven's walls are electrically immaculate.
3. Water is not compressible
4. The gravitational effect is disregarded
5. The transfer of mass is insignificant. As the water is heated further, it eventually reaches 100 degrees Celsius and begins to boil, evaporate, and release heat as vapor into the atmosphere. The phase transitions are disregarded.

2. Mesh

In this step, the user configures the mesh and free tetrahedral meshes with precise element size are used to construct the model. 265787 domain elements, 13518 boundary elements, and 827 edge elements comprise the complete mesh. The assessment of the lattice

element's quality is illustrated in Figure 2. An increase in mesh fineness corresponds to a higher quality. Therefore, the subsequent computations will be supported by dependable meshes (Lee, 2024b).

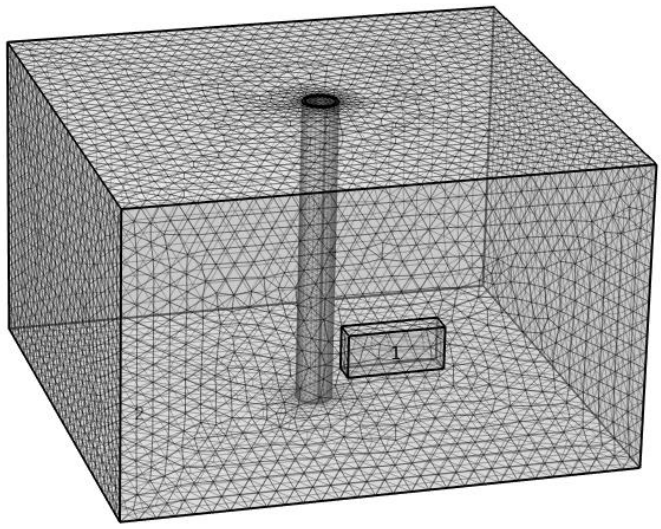

Fig 2. An evaluation of mesh element quality

Result and Discussion

1. Effect of Electromagnetic power generation

The electromagnetic powers generated to the water stream comprised to the model employed. The temperature will increase as soon as the microwave is activated and will continue to rise with time. This occurs due to the absorption of electromagnetic energy by water, which causes it to heat up. The consequence of these outcomes is temperature variation in the water, which facilitates convection. The electric field predominantly manifests in the water's bulk, as depicted in Figure 3. At the water's surface, the generation of electromagnetic power is determined by the electric field intensity and dielectric loss. Water absorbs a significant portion of its thermal energy from the electric field, more precisely microwaves. Analogous power generation profiles were noted as a result of the equivalent magnitude of dielectric loss ($p = 12.12$) occurring at ambient temperature in water. As the temperature rose, there was a concomitant increase in dielectric loss, which led to a more substantial heat gain due to the fluid's exposure to electromagnetic radiation within the cavity. Surprisingly, the convective flow that takes place in the water after sixty seconds does not cause a significant rise in temperature. It can be observed from Figure 4 that the water temperature is almost constant after a one-minute because all heat absorbed is equilibrium with the heat required for water evaporation.

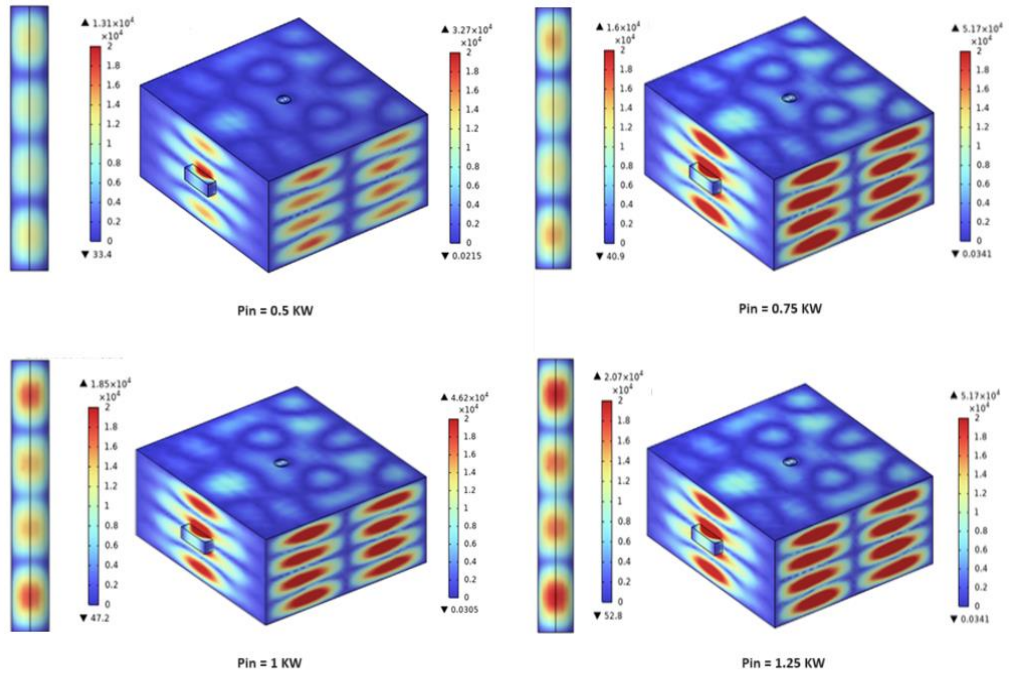

A. standard electric field (V/m)

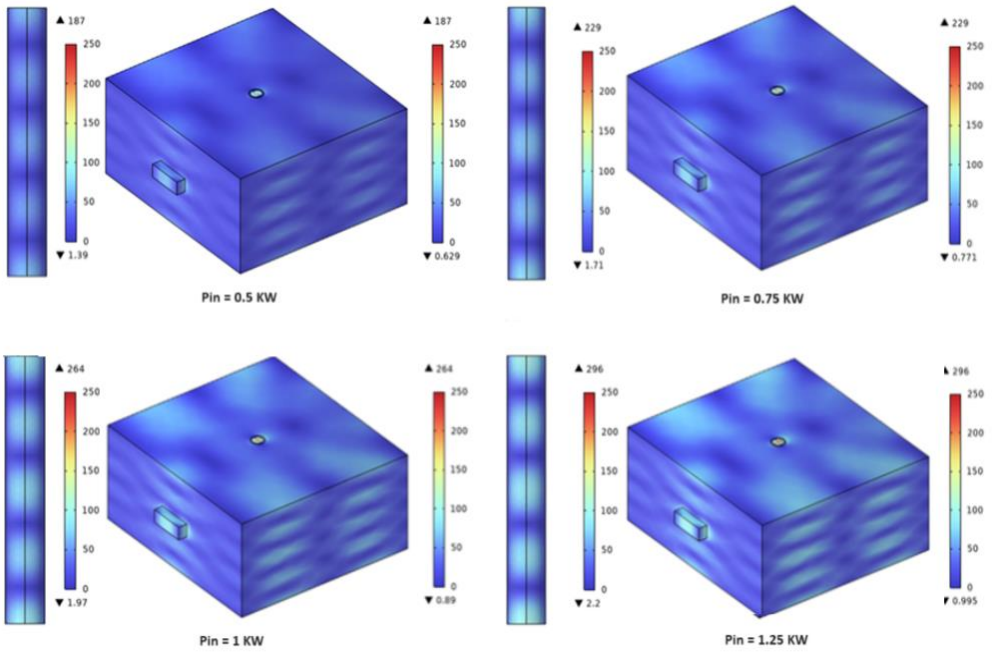

B. standard magnetic field (V/m)

Fig. 3: A. standard electric field, B. standard magnetic field (V/m)

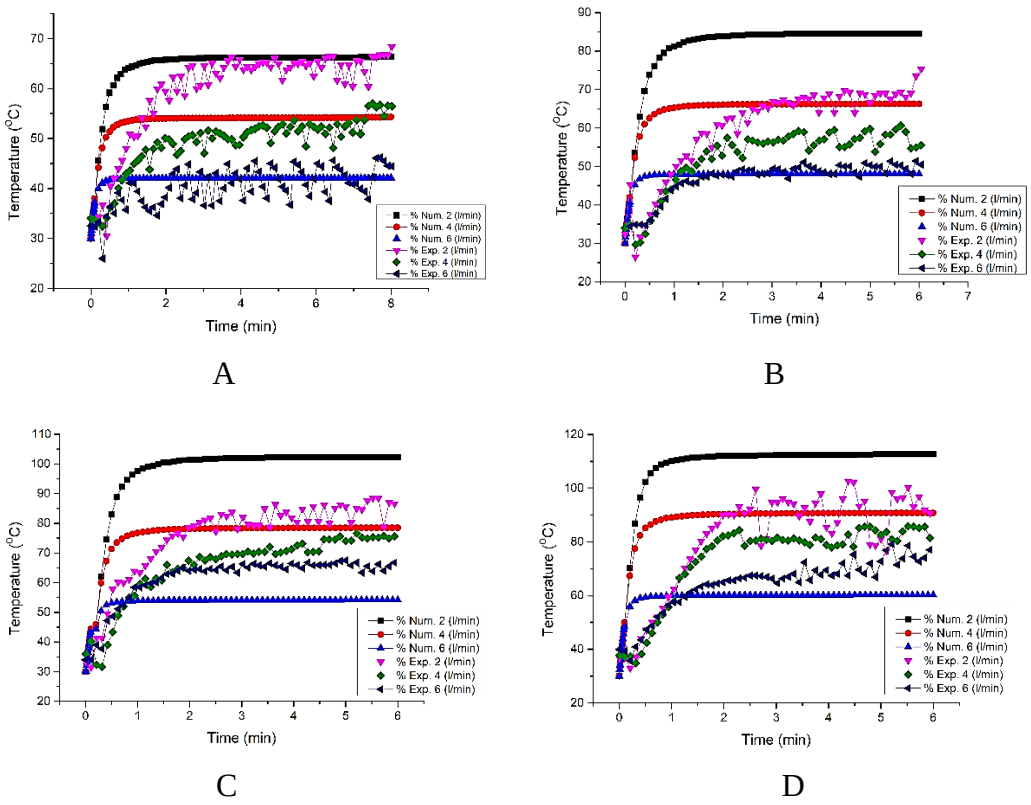

Fig 4. Comparison between experiment and model of temperature distribution at different power and flow rate A. 500 W, B. 750 W, C. 1000 W, and D. 1250 W

The analysing of the distribution of electromagnetic power densities indicates that the temperature in the upper portion of the tube is higher than the lower portion of the tube due to the flow direction from lower to upper, as illustrated in Figure 5.

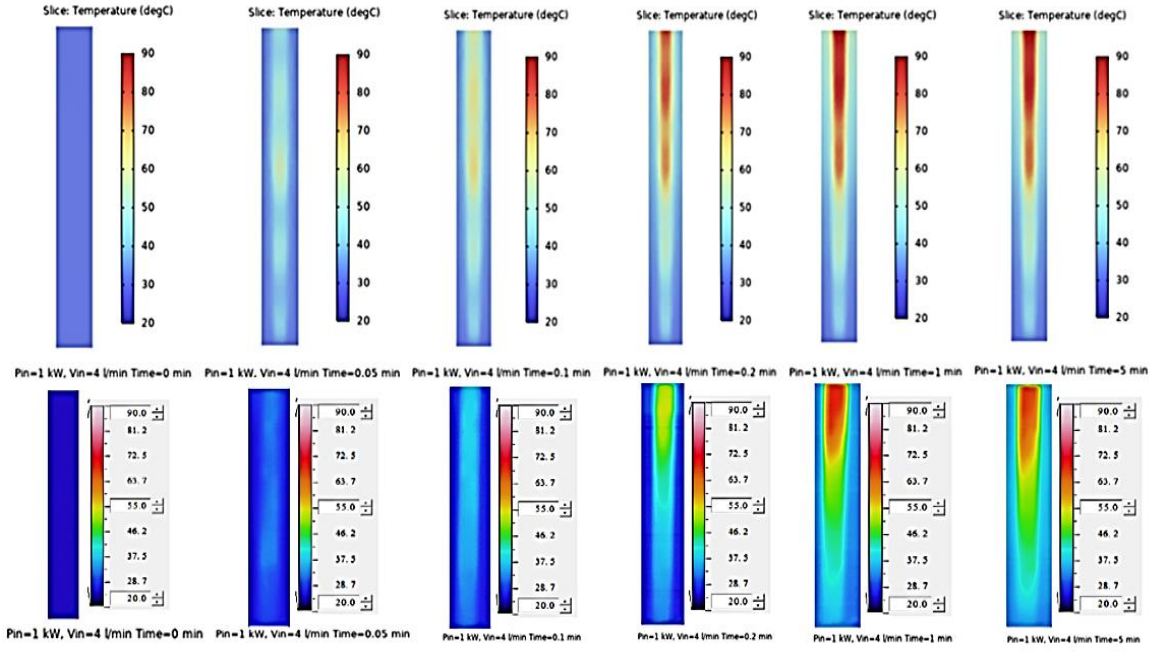

Fig. 5. A. model temperature distribution at power 1 KW and flow rate 4 l/min for different time B. experiment temperature distribution at power 1 KW and flow rate 4 l/min for different time

The water's optimum flowrate of 6 l/hr is observed near the ring-shaped tube wall at the water's surface, where heat is distributed more rapidly to the center of tube. The abrupt decrease in temperature occurred twenty seconds later. The temperature variation of the water after sixty seconds is more clearly illustrated in figure 5. Without regard to power, temperature remains constant.

At 500 W, the electric field within the microwave cavity is exceedingly feeble, and the water do not absorb sufficient energy to get the desired temperature. The electric field is observed to be stronger at 1250 W than at other power levels then the water's temperature increase caused by accelerated absorption of heat. The powerful electric field, denoted by the red region, originated in the upper portion of the tube as varied in intensity and duration of observation from the front side. The temperature distribution was obtained from all power levels as shown in figure 5.

2. Experimental Validation

To ascertain the model's validity, experiments were undertaken to quantify the increase in temperature of water when subjected to 2.45GHz radiation in microwave oven. The levels of microwave wattage are 500, 750, 1000, and 1250 W. The water temperature is recorded by infrared camera at a location within the tube, as illustrated in Figure 6. Additionally, the temperature as specified in the simulation model would be acquired at this juncture.

In the experiment, twelve sets of measurements were collected in order to generate the temperature profile. Figure 5 depicts the comparison between the experimental and simulation outcomes.

Figure 6. the Infrared camera

The experimental findings demonstrate that, the temperature rises with time. The experimental average duration of temperature increases within a 60-second while the duration is 30 second in the simulation model predicts.

Nevertheless, the prediction remains within the range of deviation of the experimental average temperature profile for the first thirty seconds. Subsequently, for the duration of the time period, the simulation output continues to fall below the acceptable threshold, albeit exhibiting a progressive increase.

The potential sources of error encompass the waveguide's physical dimensions and the potable water's quality. The capability to ascertain the electrical conductivity of the water was hindered by equipment failure. Water's dielectric constant and dielectric loss would be significantly affected by the presence of ions. The microwave will induce excitation in these ions, resulting in the production of additional thermal energy and a subsequent increase in temperature.

Aiming for an approximation of the waveguide's dimensions during model development is predicated on the physical microwave oven. Without disassembling the apparatus, an exact measurement of the waveguide could not be obtained. This may have contributed in part to the inconsistencies observed in the simulation outcomes.

the theoretical analysis conclude that the heat generation was equilibrium with heat loss after 30 sec. The temperature fluctuations of the liquid throughout the heating process could be recorded by a thermal imaging infrared camera which experimentally show that heat is consistently produced. The temperature difference under continuous heating conditions can be predicted using this model, as depicted in Figure 4.

The anticipated temperature values would marginally surpass the experimental values within the acceptable range of variation. In situations where the experimental outcomes are further validated through the utilization of thermal imaging technology. As a result, the current study will continue to employ the pulsed configuration to examine the impact of power of microwave heating.

3. Comparison between experimental and simulated temperature data

Figure 4 illustrates a comparison between the mean temperatures obtained experimentally and those obtained from simulations for each power and flow rate. A perceptible degree of concurrence was detected between the mean values obtained from the simulation and the experimental results, as indicated by the linear correlation slope. A consistent deviation from the linear correlation between experimental and numerical values was observed.

Our hypothesis posits that the turbulent flow region generated recurrent evaporation. Practically, the turbulence increase caused by the phase change could be quite substantial, accelerating experimental equilibration beyond what numerical analysis predicted. Although phase change was integrated into the numerical model, the inherent limitations of the step-by-step approach to phase change may have compromised its ability to capture these phenomena.

To obtain a comprehensive understanding of temperature profiles at different longitudinal positions, experimental and simulated cross-sectional temperature profiles for water at all conditions were done (refer to Figure 4). In general, the experimental and numerical profiles suggested that the area with the highest temperature was located proximity close to the center. The temperature distribution influenced directly by the electromagnetic power density distribution, leading to a relatively low temperature at the tube's periphery and a high temperature in the center of tube for both experimental and numerical results (see Figure 5).

The correspondence between the experimental and the simulated temperature was deemed adequate (see Figure 4). The electromagnetic density profiles of the model exerted a direct influence on both the experimental and numerical temperature profiles of water. Specifically, these profiles led to an increase in temperature at the center and the periphery of the tube.

The electromagnetic power output at 500 W and 750 W, the temperature profile predictions generated by the model at a flow rate of 6 l/hr exhibited a high degree of concordance with the empirical data. Overall, the power generation values of 750 W, 1000 W, and 1250 W the temperature predicted by the model is higher than experimental data. The potential effect on the simulated temperatures and increased power generation could have been attributed to the implementation of a larger lattice size. The rationale for selecting the larger mesh size was to examine the potential for iterative coupling between electromagnetism and fluid flow, heat transfer, and phase change in COMSOL Multiphysics for both Newtonian and non-Newtonian fluids, which was the main purpose of the study.

It is apparent that the experimental results and the simulation outcomes that exhibit a high degree of concurrence was calculated, thus validating the dependability of the model. The slight discrepancies that were noted may be attributed to the thermal dissipation process. There are various factors that can pose challenges to the effective absorption of microwave energy in experiments, such as microwave leakage and reflection. On the contrary, the process becomes more idealized during the simulation phase.

Conclusion

This research outlines the construction of a simulation model that implements microwave heating with continuous flow of water. The model integrates iterative coupling of high frequency electromagnetism, fluid flow, and heat transmission over Newtonian and non-Newtonian fluids and makes use of the COMSOL Multiphysics software application. The apparent specific heat method was employed to incorporate phase change as a phenomenon into the model.

The empirical support for the hypothesis that electricity generation was influenced by the dielectric properties of the liquid was provided by the model. A comprehensive validation of the model was conducted by utilizing experimental data acquired through the implementation of an infrared camera.

The temperature in the center of tube is higher than the temperature at the periphery. The temperature of the fluid increases with decreasing of the flow rate. The temperature increases with increasing the microwave power.

The electromagnetic power output demonstrated significant variation, spanning from 500 W to 750 W. Furthermore, the temperature profile predictions produced by the model, assuming a flow rate of 6 l/hr, aligned closely with the empirical data. In general, the power generation values of 750 W, 1000 W, and 1250 W exceeded the predictions derived from experimental data. As a result of memory constraints on the computer, it was not feasible to decrease the geometry size of the iterative model. The application of the numerical model has the potential to optimize the microwave heating procedure in the future by enhancing comprehension of the microwave heating process involving continuous flow (Castellani, 2023). Further experimental investigation is required in order to validate the simulation model.

References

Ahmed, M., & Theydan, S. (2014). Fluoroquinolones antibiotics adsorption onto microporous activated carbon from lignocellulosic biomass by microwave pyrolysis. *Journal of the Taiwan Institute of Chemical Engineers*, *45*, 219–226. https://doi.org/10.1016/j.jtice.2013.05.014

Al-Mashhadani, M. K. H., Hadi, S. M., Abed, K. M., & Hassan, H. A. (2023). The Thermal Pre-Processing Technique of the Bio-Waste for Contaminated Water Treatment: Histological and Experimental Study. *Iranian Journal of Chemistry and Chemical Engineering*, *42*(1), 349–360. https://doi.org/10.30492/IJCCE.2022.548105.5160

al-okbi, Y., Al-Anssari, S., Al-murshedi, A., Ibrahim, S., & Al-Dujele, R. (2021). Simulation and experimentation study on the performance of metal hydride storage vessels. *International Journal of Energy Research*, *46*. https://doi.org/10.1002/er.7420

Cao, H., Fan, D., Jiao, X., Huang, J., Zhao, J., Yan, B., Zhou, W., Zhang, W., & Zhang, H. (2018). Effects of microwave combined with conduction heating on surimi quality and morphology. *Journal of Food Engineering*, *228*, 1–11. https://doi.org/https://doi.org/10.1016/j.jfoodeng.2018.01.021

Castellani, F. (2023). Advanced Methods for Wind Turbine Performance Analysis Based on SCADA Data and CFD Simulations. *Energies*, *16*(3). https://doi.org/10.3390/en16031081

Chan, C.-H., Yusoff, R., & Ngoh, G.-C. (2014). Optimization of microwave-assisted extraction based on absorbed microwave power and energy. *Chemical Engineering Science*, *111*, 41–47. https://doi.org/https://doi.org/10.1016/j.ces.2014.02.011

Gao, X., Liu, X., Yan, P., Li, X., & Li, H. (2019). Numerical analysis and optimization of the microwave inductive heating performance of water film. *International Journal of Heat and Mass Transfer*, *139*, 17–30. https://doi.org/10.1016/j.ijheatmasstransfer.2019.04.122

Hong, Y., Lin, B., Li, H., Dai, H., Zhu, C., & Yao, H. (2016). Three-dimensional simulation of microwave heating coal sample with varying parameters. *Applied Thermal*

Engineering, *93*, 1145–1154. https://doi.org/https://doi.org/10.1016/j.applthermaleng.2015.10.041

Knoerzer, K., Regier, M., & Schubert, H. (2006). Microwave heating: A new approach of simulation and validation. *Chemical Engineering and Technology*, *29*(7), 796–801. https://doi.org/10.1002/ceat.200600038

Lee, C. (2024a). Optimal Design of a Variable-Pitch Axial Flow Fan by Applying Optimization Algorithm to Design, Through-Flow Analysis and CFD Simulation Methods. *Proceedings of the International Conference on Simulation and Modeling Methodologies, Technologies and Applications*, 363–369. https://doi.org/10.5220/0012798200003758

Lee, C. (2024b). Optimal Design of a Variable-Pitch Axial Flow Fan by Applying Optimization Algorithm to Design, Through-Flow Analysis and CFD Simulation Methods. *Proceedings of the 19th International Conference on Software Technologies, ICSOFT 2024*, 363–369. https://doi.org/10.5220/0012798200003758

Li, H., Liu, J., Li, X., & Gao, X. (2019). Microwave-induced polar/nonpolar mixture separation performance in a film evaporation process. *AIChE Journal*, *65*(2), 745–754. https://doi.org/10.1002/aic.16436

Liang, F., Zhu, Y., Ye, T., Jiang, S., Lin, L., & Lu, J. (2020). Effect of ultrasound assisted treatment and microwave combined with water bath heating on gel properties of surimi-crabmeat mixed gels. *Lwt*, *133*(193), 110098. https://doi.org/10.1016/j.lwt.2020.110098

Maaroof, A. A. (2024). A New Air-Assisted Flare Tip Design for Managing Gas Flare Emissions (CFD Analysis). *Processes*, *12*(9). https://doi.org/10.3390/pr12091834

Ohkubo, M., Osatomi, K., Hara, K., Ishihara, T., & Aranishi, F. (2005). Myofibrillar proteolysis by myofibril-bound serine protease from white croaker Argyrosomus argentatus. *Fisheries Science*, *71*(5), 1143–1148. https://doi.org/10.1111/j.1444-2906.2005.01074.x

Salvi, D., Boldor, D., Aita, G. M., & Sabliov, C. M. (2011). COMSOL Multiphysics model for continuous flow microwave heating of liquids. *Journal of Food Engineering*, *104*(3), 422–429. https://doi.org/10.1016/j.jfoodeng.2011.01.005

Vencels, J., Birjukovs, M., Kataja, J., & Råback, P. (2019). Microwave heating of water in a rectangular waveguide: Validating EOF-Library against COMSOL multiphysics and existing numerical studies. *Case Studies in Thermal Engineering*, *15*(August), 100530. https://doi.org/10.1016/j.csite.2019.100530

Vencels, J., Råback, P., & Geža, V. (2019). EOF-Library: Open-source Elmer FEM and OpenFOAM coupler for electromagnetics and fluid dynamics. *SoftwareX*, *9*, 68–72. https://doi.org/https://doi.org/10.1016/j.softx.2019.01.007

Yeong, S. P., Law, M. C., Vincent Lee, C. C., & Chan, Y. S. (2017). Modelling batch microwave heating of water. *IOP Conference Series: Materials Science and Engineering*, *217*(1). https://doi.org/10.1088/1757-899X/217/1/012035

Zhang, Q. (2024). Integrated CFD and MBD methods for dynamic performance analysis of a high-speed train transitioning through varied windbreak corridor designs. *Journal of Wind Engineering and Industrial Aerodynamics, 250*. https://doi.org/10.1016/j.jweia.2024.105755